Available online at www.sciencedirect.com
ScienceDirect
Bioorganic & Medicinal Chemistry 14 (2006) 7816–7825
Bioorganic & Medicinal Chemistry

Biotinylated biphenyl ketone-containing 2,4-dioxobutanoic acids designed as HIV-1 integrase photoaffinity ligands

Xue Zhi Zhao,[a] Elena A. Semenova,[b] Chenzhong Liao,[a] Marc Nicklaus,[a] Yves Pommier[b] and Terrence R. Burke, Jr.[a,*]

[a]*Laboratory of Medicinal Chemistry, CCR, NCI, NIH, Frederick, MD 21702, USA*
[b]*Laboratory of Molecular Pharmacology, CCR, NCI, NIH, Bethesda, MD 20892, USA*

Received 16 June 2006; revised 28 July 2006; accepted 29 July 2006
Available online 26 September 2006

Abstract—The diketo acid (DKA) class of HIV-1 integrase inhibitors are thought to function by chelating divalent metal ions within the enzyme catalytic center. However, differences in mutations conferring resistance among sub-families of DKA inhibitors suggest that multiple binding orientations may exist. In order to facilitate identification of DKA-binding sites, biotin-tagged biphenyl ketone-containing 2,4-dioxobutanoic acids were prepared as DKA photoaffinity probes. Introduction of biotin was obtained by means of Huisgen [3+2] cycloaddition 'click chemistry.' Two photoprobes, **5a** and **5b**, were prepared bearing short and long linker segments, respectively, between the biotin and DKA nucleus. The greatest inhibitory potency was shown by **5b**, which inhibited 3′-processing and strand transfer reactions with IC_{50} values of >333 μM and 12.4 μM, respectively. In cross-linking assays designed to measure disruption of substrate DNA binding, the photoprobes behaved similarly to a reference DKA inhibitor. Analogues **5a** and **5b** represent novel photoaffinity ligands, which may be useful in clarifying the HIV-1 binding interactions of DKA inhibitors.
Published by Elsevier Ltd.

1. Introduction

Integrase (IN) is an essential enzyme in the viral life cycle of HIV-1, the causative agent of acquired immunodeficiency syndrome (AIDS).[1] IN functions by catalyzing the insertion of virally transcribed DNA into the host genome in a two-stage process. In the first step, termed '3′-processing' (3′-P), a GT dinucleotide pair is cleaved from the viral cDNA 3′-terminus. Placement of this processed cDNA into the host genome occurs in a second step referred to as 'strand transfer' (ST).[2] Inhibitors of IN have been the object of intense development due to their potential utility as new therapeutics for the treatment of AIDS.[2–5] Although a large number of structurally diverse IN inhibitors have been reported, in cellular HIV infection assays many of these fail to provide cytoprotection or target processes other than integration.[6] An exception is provided by diketo acid inhibitors (DKA), which can afford good antiviral efficacy and exhibit potent inhibition of IN in whole cells as well as in extracellular assays.[7] DKA inhibitors are exemplified by 4-aryl-2,4-dioxobutanoic acids such as **1**[8] and **2**,[9] and non-carboxylic acid-containing analogues such as 5-CITEP (**3**)[10] as well as a variety of other analogues that contain imbedded heteroatoms, which replace aspects of the dioxobutanoic acid functionality (**4**,[11] Fig. 1). Evidence suggests that these inhibitors chelate divalent Mg^{2+} ions that are held in the IN active site by a conserved triad of acidic residues Asp64, Asp116, and Glu152, termed the 'DDE' motif.[2,12] In spite of their shared structural features and proposed common mechanism of action, data from resistant mutants[13] as

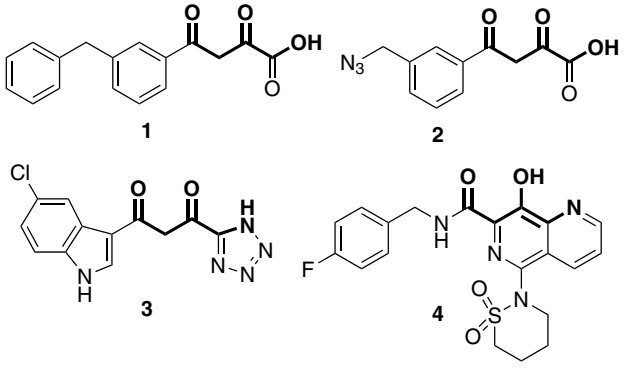

Figure 1. DKA class HIV-1 IN inhibitors with functionally equivalent diketo acid-derived substructures in bold.

Keywords: HIV-1 integrase; Inhibitor; Biotin; Photoaffinity.
* Corresponding author. Tel.: +1 301 846 5906; fax: +1 301 846 6033; e-mail: tburke@helix.nih.gov

0968-0896/$ - see front matter Published by Elsevier Ltd.
doi:10.1016/j.bmc.2006.07.064

well as computational studies[14] indicate that distinct binding sites may be involved with different subclasses of DKA inhibitors. Accordingly, direct determination of DKA-binding sites under physiologically relevant conditions is needed.

Photoaffinity labeling represents a highly useful means of identifying sites of molecular interactions.[15] This technique relies on incorporation into the ligand of interest of chemical functionality that is inert until specific light activation. Among several potential photo-reactive groups that include diazirines and aryl azides, the benzophenone moiety (BP) has proven to be advantageous[16] because of its chemical stability and unreactivity toward ambient light (activation is achieved at wavelengths in the range 350–360 nm). Additionally, once photo-activated BP groups react preferentially with C–H bonds, even under aqueous conditions.

We have previously reported the incorporation of BP groups into coumarin-based IN inhibitors[17] and these agents have recently been used to identify a putative coumarin binding site on the IN protein.[18] Using a similar approach we set out to identify binding sites associated with the DKA inhibitors. For this purpose, we designed photoprobes that utilized a BP moiety both as part of the photophore and simultaneously as a critical component of the DKA pharmacophore.[19] However, the use of these inhibitors as photoaffinity ligands is potentially limited by low cross-linking efficiency that results in high background noise. Such drawbacks could be overcome by including biotin as part of the photoaffinity ligand to facilitate selective purification of covalent adducts.[15] Biotin tagging of phenylazide,[20] diazirine,[21] and BP-containing photoprobes[22–24] has proven to be useful in other systems. In the current report, we detail the application of biotin tagging to the design and synthesis of BP-containing DKA photoprobes as potential tools for identifying binding sites of DKA-based IN inhibitors.

2. Results and discussion

2.1. Design and synthesis of biotin-tagged photoprobes

Recent examples of large biotin-tagged affinity ligands have appeared in which the biotin residue is situated at some distance from the photophore functionality.[23,24] However, DKA photoprobes are structurally simple and can consist of nothing more than a biphenyl ketone moiety and a diketo acid side chain.[19] For such compounds, introduction of biotin through a linker onto the 4-position of the BP ring system results in trifunctional analogues of type **5** (Fig. 2). We envisioned construction of the necessary 'linker' segments using Huisgen [3+2] azide–alkyne cycloaddition-mediated 'click chemistry.'[25,26] Similar methodology has proven useful in the biotin tagging of other photophore-containing ligands.[27] Based on this approach, targets **5a** and **5b** were designed, which differ in the length of their cycloaddition-derived triazole-containing linker segments (Fig. 2).

Preparation of **5a** and **5b** required the synthesis of the common intermediate azide **13** (Scheme 1). The route began by coupling commercially available 4-methylbenzaldehyde (**6**) with 1,3-dibromobenzene (**7**) in the presence of *n*-BuLi to yield the biphenylmethyl alcohol **8** (Scheme 1).[8] Further reaction with *n*-BuLi followed by addition of *N*-methoxy-*N*-methylacetamide provided the methyl ketone **9**. This was subjected to Collins oxidation to give the diketone **10** (59% overall yield from **6**).[28,29] Heating **10** with *N*-bromosuccinimide (NBS) in the presence of dibenzoyl peroxide[30] resulted in selective benzylic bromination to provide intermediate **11**. This was reacted with sodium azide to yield **12** (60% yield from **10**). Condensation of the aryl methyl ketone **12** with diethyl oxalate using either lithium bis(trimethylsilyl)amide (LHMDS) in THF at −20 °C or sodium hydride in toluene at reflux[31] gave the diketo ester **13** in 32% yield following HPLC purification. The photoaffinity probe **14** was prepared by deprotecting ester **13** using lithium hydroxide in THF and H_2O. The intermediate **10** was converted to the diketo acid ester **15** and hydrolyzed to yield the photoprobe **16** (Scheme 2).

The commercially available *N*-hydroxysuccinimide active ester of biotin (**17a**)[32] was dissolved in DMF and to this was added neat propargylamine followed by an aqueous solution of sodium bicarbonate to afford the alkyne **18a** (Scheme 3). Similar reaction using the chain-extended analogue **17b**[32] gave the corresponding propargylamide **18b**. Initial attempts at Huisgen Cu(I)-catalyzed [3+2] cycloaddition of **18a** with the azide-containing β-diketoacid ethyl ester **13** in the absence of a

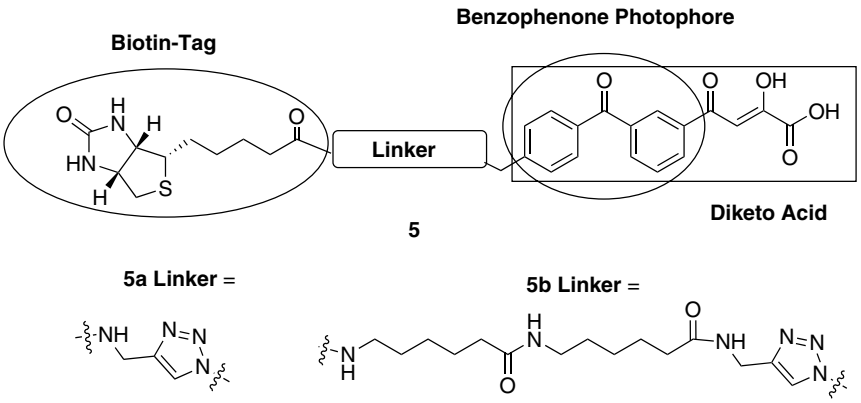

Figure 2. Structures of biotin-tagged BP-containing DKA photoprobes.

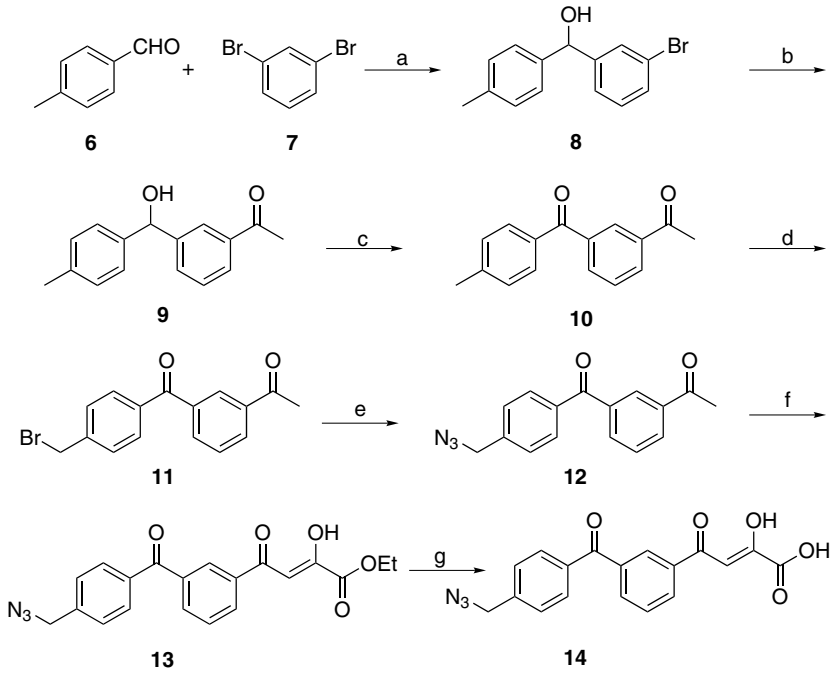

Scheme 1. Reagents and conditions: (a) **7**, *n*-BuLi, THF, −78 °C, then **6**, −78 °C to rt (79% yield); (b) *n*-BuLi, THF, −78 °C, then *N*-methoxy-*N*-methylacetamide, −78 °C to rt (79% yield); (c) CrO_3, pyridine, CH_2Cl_2, 0 °C (94% yield); (d) NBS, benzoyl peroxide, CCl_4, reflux (70% yield); (e) NaN_3, acetone/H_2O (5:1), reflux (85% yield); (f) LHMDS, THF, −20 °C, then $(CO_2Et)_2$ (32% yield); (g) LiOH·H_2O, THF/H_2O, rt (85% yield).

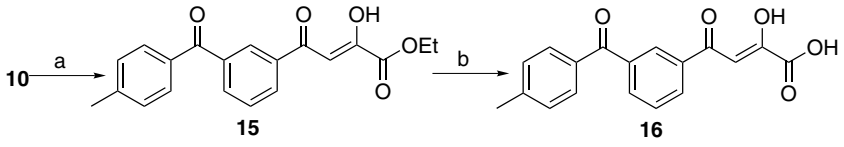

Scheme 2. Reagents and conditions: (a) LHMDS, THF, −78 °C, then $(CO_2Et)_2$, (78% yield); (b) LiOH·H_2O, THF/H_2O (82% yield).

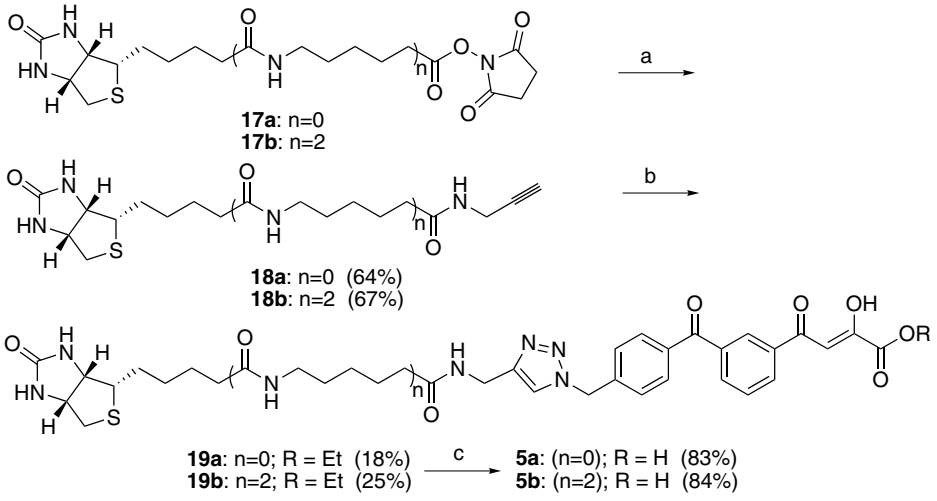

Scheme 3. Reagents and conditions: (a) propargylamine, $NaHCO_3$ (aq), DMF; (b) **13**, (+)-sodium L-ascorbate, $CuSO_4·5H_2O$, DIPEA, $^tBuOH/H_2O$, rt; HPLC purification; (c) LiOH·H_2O THF/H_2O; HPLC purification.

nitrogen base failed to give good results, even after extended reaction times.[26] However, inclusion of diisopropylethylamine (DIPEA) in the reaction mixture improved the reaction[33] and the 1,4-substituted triazole-containing adduct **19a** was obtained in 18% yield after HPLC purification. Hydrolysis of the ethyl ester followed by HPLC purification yielded the final biotin-tagged DKA photoprobe **5a** in 83% yield. A similar series of reactions applied to the linker-elongated propargylamide **18b** gave the desired photoprobe **5b**.

2.2. Evaluation of inhibitory potencies against HIV-1 integrase

Synthetic compounds were examined for their ability to inhibit HIV-1 IN using in vitro assays in the presence of Mg^{2+} as the metal cofactor.[34] [γ-^{32}P]-Labeled 21 base pair (bp) oligonucleotide duplexes corresponding to the terminal U5 sequence of the HIV-1 LTR were used as substrate. Cleavage of two bases during 3′-P resulted in 19-bp products, while strand transfer products (STP) were formed by covalent joining of the 19-bp sequences into identical duplexes that further served as target DNA. Reactions were run at 37 °C in the presence of various concentrations of inhibitors. Analysis was done by gel electrophoresis and PhosphorImager visualization. Bands corresponding to 19-bp 3′-P products as well as STP bands were quantitated and plotted to provide inhibition constants for both the 3′-P and ST reactions. A tabulation of IC_{50} values obtained in this fashion is shown in Table 1.

Because the biotin-labeled photoprobes **5a** and **5b** were designed to tag relevant DKA sites, it was of interest to examine whether the biotin and linker appendages unduly perturbed DKA binding. One characteristic of many DKA inhibitors is the selective inhibition of ST reactions relative to 3′-P reactions. For compound **2**,[9] which represents a reference DKA lacking any BP functionality or biotin-linker appendages, ST selectivity was approximately 50-fold. High ST selectivity was also observed for BP-containing DKA inhibitors **14** and **16**, which lack biotin and linker moieties. Biotinylated photoprobe **5a** bearing a relatively short linker segment exhibited significantly reduced ST selectivity (approximately 3-fold selectivity). However, by increasing the length of the linker segment, photoprobe **5b** regained the lost ST selectivity and underwent an increase in inhibitory potency.

Table 1. Inhibitory potencies of synthetic analogues calculated from in vitro HIV-1 integrase assays

Compound	$IC_{50} \pm SE$[a] (μM)	
	3′-P	ST
2	43.6 ± 27.3	0.76 ± 0.24
16	>333	14.0 ± 9.4
14	>333	33.7 ± 18.9
5a	136.7 ± 9.8	40.7 ± 23.3
5b	>333	12.4 ± 5.7

[a] Values represent the averages of three independent experiments conducted as described in Ref. 34.

Compound **5b** exhibited ST inhibitory potency and selectivity over 3′P very similar to compound **16**, which was unencumbered by any biotin-linker appendage. This potentially indicates that the biotin-linker functionality in **5b** does not unduly perturb binding. Additionally, although the inhibitory potency of **5b** (ST IC_{50} = 12.4 μM) is reduced relative to the parent DKA inhibitor **2** (ST IC_{50} = 0.76 μM), it is similar to the potency of a BP-containing inhibitor (ST IC_{50} = 10 μM)[17] that was recently used to identify a novel IN binding site.[18]

2.3. Inhibitor effects on binding of DNA to integrase

In addition to changing ST selectivity, alterations in the binding of the biotin-tagged photoprobes to IN may differentially affect binding of DNA. To examine effects of inhibitors on the binding of DNA within the catalytic site, a disulfide cross-linking assay was run as depicted in Figure 3. This assay utilized DNA substrate having

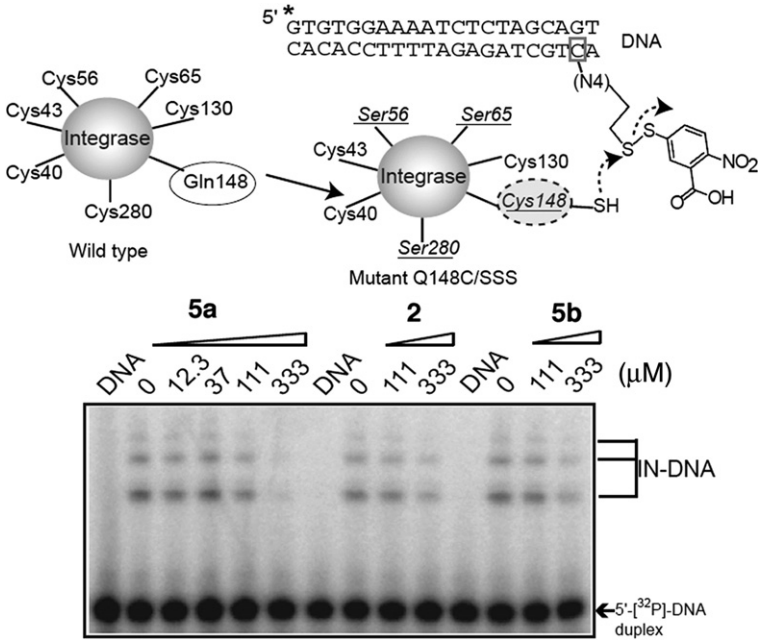

Figure 3. Results of IN–DNA disulfide cross-linking assay performed as reported in Ref. 34. (Top left) Schematic representation showing HIV-1 IN cysteine (Cys) residues. (Top right) Mutant IN along with cross-linking strategy. Asterisk represents the 5′ ^{32}P-label. (Bottom) SDS–PAGE analysis showing the effects of increasing concentrations of inhibitors (shown above the gel) on formation of cross-linked IN–DNA.

a 5′-AC cystosine residue that was modified to include thiol-reactive functionality appended to its N4 position. Mutant IN was used, which contained a Q148C mutation in the flexible loop proximal to the catalytic site. Other reactive Cys residues within the IN protein were converted to non-reactive Ser residues so that disulfide cross-linking of the DNA only occurred with the Cys148 residue.[35] As shown in Figure 3, parent DKA inhibitor **2** as well as **5a** and **5b** inhibit DNA–IN cross-linking only at concentrations significantly higher than their ST IC_{50} values.

A second experiment was run to measure effects of inhibitors on overall binding of DNA to IN. The assay employed DNA that mimicked the viral U5 LTR and contained an abasic site corresponding to the adenine in the conserved terminal CA-dinucleotide (Fig. 4). Nitrogen nucleophiles within the IN protein can form Schiff-bases with the abasic C1′-hemiacetal. Subsequent in situ reduction using $NaBH_4$ results in irreversible cross-linking of the DNA to the IN.[36] Results of this assay indicated that the parent DKA inhibitor **2** as well as the biotin-tagged photoprobes **5a** and **5b** behaved similarly in not affecting the overall binding of DNA at concentrations within the range needed to inhibit ST catalysis (Fig. 4). Significant inhibition of DNA binding was observed for photoprobe **5a** at 333 μM, however this was well above its ST inhibitory concentration of 40.7 μM.

2.4. Molecular modeling studies

To examine whether reasonable binding modes to IN were possible for **5a** and **5b**, docking calculations were carried out using a structural model of the full-length HIV-1 IN dimer complexed with donor DNA.[37] As pointed out above, mutations conferring resistance to DKA inhibitors map to the enzyme active site proximal to catalytic residues Asp64, Asp116, and Glu152.[7] Consistent with this, in the current study automated docking of inhibitors preferentially situated them close to the active site, even through a broad search region was employed and differences did exist between the highest scored poses of inhibitors. It is widely assumed that DKA inhibitors function by chelating one or two Mg^{2+} ions required for productive catalysis. Figure 5 overlays the best scoring pose for **5a** and **5b** in which the diketo acid groups chelate a Mg^{2+} ion. Figure 6 provides an overall visual inspection of **5a** and **5b** bound to the full-length IN–DNA complex. We chose to present these highest-scored poses even though they are quite different looking and might suggest different binding models for **5a** and **5b** at first glance. However, as is well known, scores calculated by docking programs are at best semi-quantitative and do not usually permit exact reproduction of ranking of assayed compounds. Therefore, we could have 'hand-picked' poses for **5a** and **5b** that look much more similar to each other, albeit at the cost of introducing our bias into the reported results.

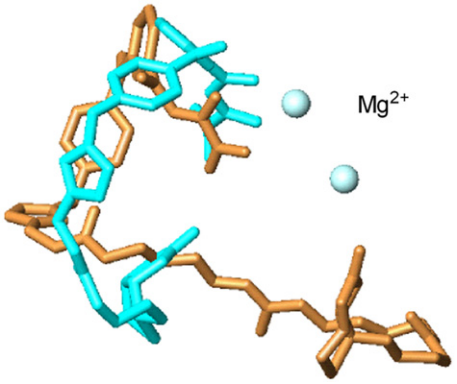

Figure 5. Overlapped binding modes of **5a** (khaki) and **5b** (cyan).

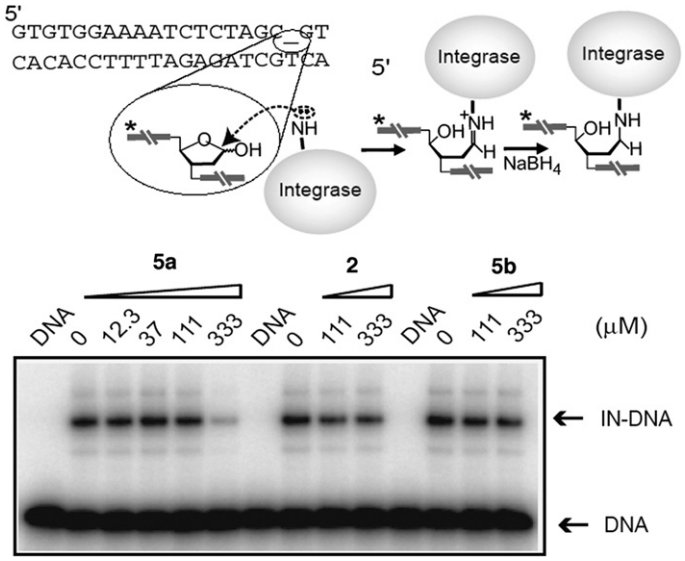

Figure 4. Results of IN–DNA Schiff-base cross-linking assay as performed in reference 36. (Top) Assay schematic showing imine formation between an abasic site in the DNA substrate and an amine nucleophile from the IN protein (left), with subsequent $NaBH_4$ reduction to the amine cross-linked product (right). Asterisk represents the 5′ ^{32}P-label. (Bottom) SDS–PAGE showing effects of increasing inhibitor concentrations on formation of IN–DNA cross-linked product.

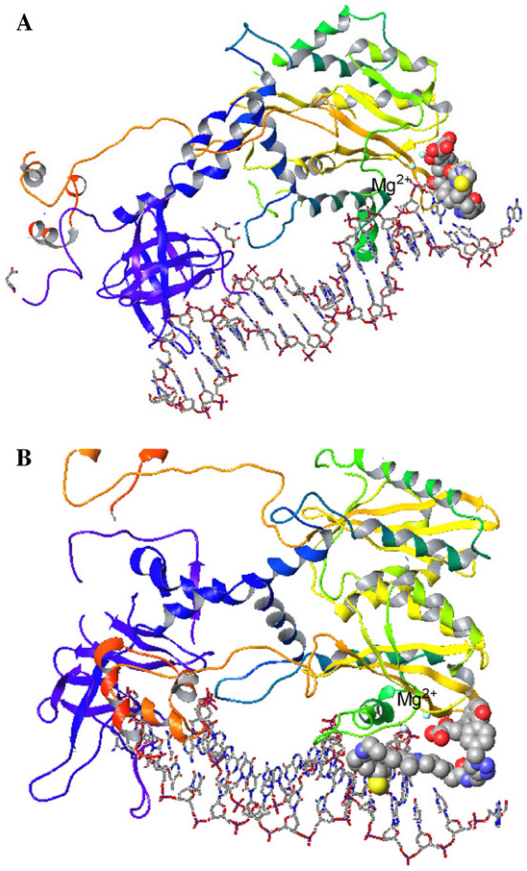

Figure 6. Hypothetical binding of **5a** (A) and **5b** (B) to a model of full-length IN complexed with donor DNA. Protein coloring is rendered in gradations from blue to red proceeding from the N-terminus to the C-terminus, respectively.

The key conclusion of these molecular modeling studies is that inhibitors **5a** and **5b** can be reasonably accommodated in the IN–DNA complex.

In conclusion, the current work has resulted in biotin-tagged BP-containing DKAs that were prepared using Huisgen [3+2] cycloaddition 'click chemistry.' Two photoprobes were obtained that differed in the length of the segment joining the biotin to the BP ring system. Analogue **5a**, which contained a short linker segment, exhibited reduced selectivity toward ST inhibition relative to 3′-P and at higher doses it inhibited total DNA binding. Analogue **5b** contained a longer linker segment and it showed selective inhibition of ST reactions that was comparable to an analogue (**16**), which lacked any biotin or linker functionality. Analogues **5a** and **5b** represent novel photoaffinity probes that may be useful in studying the binding of DKA inhibitors to IN. Such work is currently in progress and will be reported elsewhere.

3. Experimental

3.1. Biological evaluation

Experimental conditions for all biological procedures have been previously reported.[34]

3.2. Docking experiments

Docking studies of compounds listed in Table 1 were performed on a structural model of the full-length HIV-1 IN dimer complexed with an oligonucleotide corresponding to the U5 LTR.[37] Experiments were performed using the program Glide 4.0, which is part of the First Discovery suite (Schrödinger Inc.).[38] Coordinates of the full-length substrate-complexed dimer were prepared for Glide 4.0 calculations by running the First Discovery suite scripts *pprep* and *impref*. The *pprep* script produces a new receptor file in which all residues are neutralized except those that are relatively close to the ligand (if the protein is complexed with a ligand) or form salt bridges. The *impref* script runs a series of restrained impact energy minimizations using the Impact utility. Minimizations were run until the average root mean square deviation (rmsd) of the non-hydrogen atoms reached 0.3 Å. In order to study the binding modes of inhibitors in the presence of metal ions, grid files were generated representing the shape and properties of the receptor including Mg^{2+} in the active site. Glide uses two boxes that share a common center to organize its calculations: a larger enclosing box and a smaller binding box. The grids themselves are calculated within the space defined by the enclosing box. The binding box defines the space through which the center of the defined ligand will be allowed to move during docking calculations. It provides a measure of the effective size of the search space. The only requirement on the enclosing box is that it be large enough to contain all ligand atoms, even when the ligand center is placed at an edge or vertex of the binding box. Grid files were generated with catalytic residues Asp64, Asp116, and Glu152 at the center of the two boxes. The size of the binding box was set at 20 Å in order to explore a large region of the protein. The three-dimensional structures of the compounds **2**, **5a**, **5b**, **14**, and **16** were constructed using ISIS/Draw and imported into the Maestro interface. The initial geometry of the structures was optimized using the OPLS-2005 force field[39] performing 1000 steps of conjugate gradient minimization. The compounds were subjected to flexible docking using the pre-computed grid files. For each compound the 100 top-scored poses were saved and analyzed.

3.3. Chemistry

High-resolution mass spectra (HRMS) were obtained from UCR Mass Spectrometry Facility, University of California at Riverside and fast-atom bombardment mass spectra (FABMS) were acquired with a VG Analytical 7070E mass spectrometer under the control of a VG 2035 data system. FABMS matrixes used were glycerol or nitrobenzoic acid. Both ^{1}H and ^{13}CNMR data were obtained on a Varian 400 MHz instrument and are reported in ppm relative to TMS and referenced to the solvent in which they were run. IR spectra were run neat using a Jasco FT/IR-615 instrument. Solvent was removed by rotary evaporation under reduced pressure and anhydrous solvents were obtained commercially and used without further drying. Preparative high-pressure liquid chromatogaphy (HPLC) was conducted

using a Waters Prep LC4000 system having photodiode array detection and using a YMC J'sphere ODS-H80 column (250 × 20 mm ID, S-4 μm, 80 Å) at a flow rate of 10 mL/min. with binary solvent system consisting of A = 0.1% aqueous TFA and B = 0.1% TFA in acetonitrile.

3.3.1. 3-Bromo-α-(4-methylphenyl)-benzenemethanol (8). To an oven-dried 100 mL round bottom flask under argon was added a solution of *n*-butyl lithium 1.6 M in hexanes (5.53 mL, 8.85 mmol), and the solution was cooled (−78 °C) and diluted with anhydrous THF (20 mL). To this was added dropwise over 5 min 1,3-dibromobenzene (1.0 mL, 8.04 mmol) and the reaction mixture was stirred (2.5 h at −78 °C) then 4-methylbenzaldehyde (1.05 mL, 8.84 mmol) was added over 15 min and the reaction mixture was slowly warmed to room temperature (1.5 h). The reaction mixture was quenched by the addition of ice-cold H_2O (20 mL) and extracted with ether (3× 100 mL). The combined organic extract was washed with saturated aqueous $NaHCO_3$ and brine then dried over anhydrous Na_2SO_4 and evaporated to yield a colorless oil. Purification by silica gel flash chromatography (hexanes/ethyl acetate) afforded bromide **8** as a colorless oil (1.86 g, 79% yield). ^{1}H NMR ($CDCl_3$) δ 7.53 (t, 1H, J = 1.4 Hz), 7.37 (dt, 1H, J = 1.2 Hz, 6.8 Hz), 7.25 (dd, 1H, J = 8.0 Hz), 7.20–7.12 (m, 5H), 5.67 (s, 1H), 2.51 (br s, 1H), 2.33 (s, 3H). ^{13}C NMR ($CDCl_3$) δ 146.1, 140.3, 137.6, 130.3, 129.9, 129.3 (3C), 126.5 (2C), 125.0, 122.5, 75.3, 21.1. FABMS (+ve) *m*/*z* 275, 277 [MH^+-H_2].

3.3.2. 1-[3-[Hydroxy(4-methylphenyl)methyl]phenyl]-ethanone (9). To a solution of *n*-butyl lithium 1.6 M in hexanes (0.59 mL, 0.94 mmol) at −78 °C under argon was added a solution of **8** (125 mg, 0.42 mmol) in anhydrous THF (4 mL). The reaction mixture was stirred at −78 °C for 1 h, then *N*-methoxy-*N*-methylacetamide (59 μL, 0.56 mmol) was added and the reaction mixture was slowly warmed to room temperature over 1 h. The reaction mixture was quenched by the addition of ice-cold H_2O (10 mL) then extracted with ether (3× 30 mL). The combined organic extract was washed with saturated aqueous $NaHCO_3$and brine then dried over anhydrous Na_2SO_4 and evaporated to yield a colorless oil. Purification by silica gel flash chromatography (hexanes/ethyl acetate) afforded **9** as a colorless oil (80 mg, 79% yield). ^{1}H NMR ($CDCl_3$) δ 7.97 (m, 1H), 7.81–7.78 (m, 1H), 7.55–7.52 (m, 1H), 7.40–7.32 (m, 1H), 7.23–7.20 (m, 2H), 7.12–7.10 (m, 2H), 5.81 (s, 1H), 2.54 (s, 3H), 2.29 (s, 3H). ^{13}C NMR ($CDCl_3$) δ 198.2, 144.5, 140.5, 137.6, 137.2, 131.1, 129.3 (2C), 128.6, 127.3, 126.5 (2C), 126.1, 75.6, 26.6, 21.1. FABMS (+ve) *m*/*z* 241 [MH^+].

3.3.3. 1-[3-(4-Methylbenzoyl]phenyl)-ethanone (10). Chromium(III) oxide (1.47 g, 14.7 mmol) was added in several portions to a solution of pyridine (2.38 mL, 29.5 mmol) in anhydrous dichloromethane (40 mL) at 0 °C and the mixture was stirred at 0 °C (20 min). To this was added quickly a solution of **9** (588 mg, 2.45 mmol) in anhydrous dichloromethane (10 mL) and the mixture was stirred at room temperature (10 min). The resulting black product was filtered though a column of neutral aluminum oxide and the filtrate was evaporated to dryness. Purification by silica gel flash chromatography (hexanes/ethyl acetate) afforded the desired diketone product **10** as a colorless crystalline solid (545 mg, 94% yield): Mp 77.8 – 78.0 °C. ^{1}H NMR ($CDCl_3$) δ 8.30 (m, 1H), 8.13–8.11 (m, 1H), 7.93–7.91 (m, 1H), 7.69–7.66 (m, 2H), 7.56–7.52 (m, 1H), 7.27–7.24 (m, 2H), 2.60 (s, 3H), 2.41 (s, 3H). ^{13}C NMR ($CDCl_3$) δ 197.3, 195.5, 143.8, 138.4, 137.1, 134.3, 134.1, 131.5, 130.2, 129.6, 129.2, 128.6, 26.7, 21.6. FABMS (+ve) *m*/*z* 239 [MH^+]. IR υ (cm^{-1}) 1680, 1651, 1602, 1300, 923.

3.3.4. 1-[3-[4-(Bromomethyl)benzoyl]phenyl]-ethanone (11). A suspension of **10** (1.38 g, 5.80 mmol), *N*-bromosuccinimide (NBS) (1.24 g, 6.97 mmol), and benzoyl peroxide (42 mg, 0.17 mmol) in anhydrous carbon tetrachloride (150 mL) was refluxed under argon (24 h). The reaction mixture was cooled to room temperature and filtered, the filter pad was washed with carbon tetrachloride (2× 30 mL), and the combined filtrate was evaporated. The resulting residue was purified on silica gel flash chromatography to provide **11** as a colorless oil (1.29 g, 70% yield). ^{1}H NMR ($CDCl_3$) δ 8.27 (m, 1H), 8.11–8.08 (m, 1H), 7.89–7.86 (m, 1H), 7.72–7.68 (m, 2H), 7.53–7.45 (m, 1H), 7.44–7.43 (m, 2H), 4.45 (s, 2H), 2.56 (s, 3H). ^{13}C NMR ($CDCl_3$) δ: 197.0, 194.8, 142.4, 137.6, 137.0, 136.6, 133.9, 131.7, 130.3 (2C), 130.1, 129.3, 129.0 (2C), 32.0, 26.6. FABMS (+ve) *m*/*z* 317, 319 [MH^+]. IR υ (cm^{-1}) 1730, 1685, 1656, 1603, 1236.

3.3.5. 1-[3-[4-(Azidomethyl)benzoyl]phenyl]-ethanone (12). Sodium azide (391 mg, 6.02 mmol) was added to a solution of **11** (954 mg, 3.01 mmol) in acetone (15 mL) with H_2O (3 mL) and the mixture was stirred at reflux (overnight). The mixture was cooled to room temperature, concentrated, and the residue was purified by silica gel flash chromatography to provide **12** as a colorless oil (711 mg, 85% yield). ^{1}H NMR ($CDCl_3$) δ 8.31 (m, 1H), 8.16–8.13 (m, 1H), 7.95–7.92 (m, 1H), 7.79–7.77 (m, 2H), 7.58–7.53 (m, 1H), 7.43–7.41 (m, 2H), 4.45 (s, 2H), 2.60 (s, 3H). ^{13}C NMR ($CDCl_3$) δ 197.1, 195.2, 140.4, 137.8, 137.2, 136.7, 134.1, 131.8, 130.5 (2C), 129.5, 128.8, 128.0 (2C), 54.2, 26.7. FABMS (+ve) *m*/*z* 280 [MH^+]. IR υ (cm^{-1}) 2097 (N_3), 1685 (C═O), 1657, 1595, 1237.

3.3.6. 4-[3-[4-(Azidomethyl)benzoyl]phenyl]-2-hydroxy-4-oxo-2-butenoic acid ethyl ester (13). To a stirred solution of lithium bis(trimethylsilyl)amide (LHMDS), 1.0 M in THF (2.48 mL, 2.48 mmol) at −20 °C was added dropwise a solution of **12** (230 mg, 0.82 mmol) in anhydrous THF and the reaction mixture was stirred (1 h at 20 °C), then diethyl oxalate (224 μL, 1.65 mmol) was added. The reaction mixture was slowly warmed to room temperature (3 h) then quenched with ice-cold H_2O (20 mL), extracted with chloroform (3× 100 mL), and the combined organic extract was washed with dilute aqueous HCl then brine, dried over anhydrous Na_2SO_4. Filtration followed by evaporation gave a yellow oil, which was subjected to HPLC purification (linear gradient of 40% B to 100% B over 35 min; retention

time = 30.6 min) to provide **13** as a white solid following lyophilization (100 mg, 32% yield). ^{1}H NMR ($CDCl_3$) δ 8.36 (m, 1H), 8.20–8.18 (m, 1H), 8.00–7.97 (m, 1H), 7.82–7.79 (m, 2H), 7.63 (t, 1H, J = 7.6 Hz), 7.45 (d, 2H, J = 8.0 Hz), 7.07 (s, 1H), 4.45 (s, 2H), 4.38 (qt, 2H, J = 7.2 Hz), 1.38 (t, 3H, J = 7.2 Hz). ^{13}C NMR ($CDCl_3$) δ 194.9, 189.5, 170.4, 161.9, 140.6, 138.1, 136.6, 135.2, 134.6, 131.4, 130.5 (2C), 129.1, 129.0, 128.0 (2C), 98.0, 62.7, 54.2, 14.0. FABMS (−ve) *m/z* 378 [(M−H)$^-$]. HRMS calcd for $C_{20}H_{18}N_3O_5$ [MH$^+$]: 380.1246. Found: 380.1234. IR υ (cm^{-1}) 2100 (N_3), 1732 (C=O), 1703, 1665, 1595.

3.3.7. 4-[3-[4-(Azidomethyl)benzoyl]phenyl]-2-hydroxy-4-oxo-2-butenoic acid (14). To a solution of ethyl ester **13** (25 mg, 0.07 mmol) in THF (800 μL) with H_2O (400 μL) was added lithium hydroxide monohydrate (5 mg, 0.16 mmol). The reaction mixture was stirred at room temperature (1 h) then concentrated under reduced pressure and subjected directly to HPLC purification (linear gradient of 40% B to 75% B over 30 min; retention time = 22.3 min) to provide **14** as a white solid following lyophilization (15 mg, 65% yield). ^{1}H NMR (DMSO-d_6) δ 8.30 (d, 1H, J = 8.0 Hz), 8.24 (s, 1H), 7.96 (d, 1H,J = 8.8 Hz), 7.76 (d, 2H, J = 8.0 Hz), 7.71 (t, 1H, J = 7.6 Hz), 7.53 (d, 2H, J = 8.0 Hz), 7.01 (s, 1H), 4.58 (s, 2H). FABMS (−ve) *m/z* 350 [(M−H)$^-$].

3.3.8. 2-Hydroxy-4-[3-(4-methylbenzoyl)phenyl]-4-oxo-2-butenoic acid ethyl ester (15). To a stirred solution of LHMDS, 1.0 M in THF (3.0 mL, 3.0 mmol) at −78 °C was added dropwise a solution of ketone **10** (240 mg, 1.0 mmol) in anhydrous THF. The resulting mixture was stirred (1 h at −78 °C) then diethyl oxalate (271 μL, 2.0 mmol) was added and the reaction mixture was slowly warmed to room temperature (3 h). The reaction mixture was quenched with ice-cold H_2O (20 mL) and extracted with chloroform (3× 80 mL). The combined organic extract was washed with dilute aqueous HCl then brine, dried over anhydrous Na_2SO_4, and evaporated. Purification by silica gel flash chromatography using chloroform/methanol afforded product **15** as a colorless oil (266 mg, 78% yield). ^{1}H NMR ($CDCl_3$) δ 8.33 (t, 1H, J = 1.6 Hz), 8.16 (m, 1H), 7.96 (m, 2H), 7.68 (d, 2H, J = 8.0 Hz), 7.59 (t, 1H, J = 8.0 Hz), 7.27 (d, 2H, J = 8.0 Hz), 7.05 (s, 1H), 4.36 (qt, 2H, J = 7.2 Hz), 2.41 (s, 3H), 1.37 (t, 3H, J = 7.2 Hz). ^{13}C NMR ($CDCl_3$) δ 195.2, 189.6, 170.3, 161.9, 143.9, 138.7, 135.0, 134.6, 134.1, 131.0, 130.2 (2C), 129.2 (2C), 129.0, 128.9, 98.0, 62.7, 21.7, 14.0. FABMS (+ve) *m/z* 339 [MH$^+$]. IR υ (cm^{-1}) 3033, 2862, 1731, 1655, 1604.

3.3.9. 2-Hydroxy-4-[3-(4-methylbenzoyl)phenyl]-4-oxo-2-butenoic acid (16). To a solution of ethyl ester **15** (59 mg, 0.17 mmol) in THF (800 μL) with H_2O (400 μL) was added lithium hydroxide monohydrate (15 mg, 0.47 mmol). The reaction mixture was stirred at room temperature (1 h), then concentrated under reduced pressure and purified directly by preparative HPLC (linear gradient of 40% B to 70% B over 30 min; retention time = 24.6 min) to afford **16** as a white solid following lyophilization (42 mg, 82% yield). ^{1}H NMR (DMSO-d_6) δ 8.29 (dd, 1H, J = 1.2, 8.0 Hz), 8.20 (d, 1H, J = 1.2 Hz), 7.94 (d, 1H,J = 7.6 Hz), 7.70 (t, 1H, J = 7.6 Hz), 7.64 (d, 2H, J = 8.4 Hz), 7.35 (d, 2H, J = 8.4 Hz), 7.05 (s, 1H), 2.38 (s, 3H). FABMS (−ve) *m/z* 309 [(M−H)$^-$]. HRMS calcd for $C_{18}H_{14}O_5$[M$^-$]: 310.0836. Found: 310.0849.

3.3.10. Biotin propargylamide (18a). To a solution of (+)-biotin *N*-hydroxysuccinimide active ester (**17a**)[31] (78 mg, 0.23 mmol) in DMF (1.0 mL) was added propargylamine (31 μL, 0.45 mmol) and the solution was stirred at room temperature (24 h). The solution was concentrated and subjected directly to preparative HPLC purification (linear gradient of 5% B to 40% B over 25 min; retention time = 29.2 min) to afford **18a** as a white solid following lyophilization (42 mg, 64% yield). ^{1}H NMR (DMSO-d_6) δ 8.18 (t, 1H, J = 5.4 Hz), 6.37 (s, 1H), 6.30 (s, 1H), 4.25 (dd, 1H, J = 5.2 Hz, 7.6 Hz), 4.09–4.05 (m, 1H), 3.77 (dd, 2H, J = 2.4 Hz, 5.2 Hz), 3.07–3.04 (m, 1H), 3.03 (t, 1H, J = 2.4 Hz), 2.77 (dd, 1H, J = 5.2 Hz, 12.4 Hz), 2.52 (d, 1H, J = 12.4 Hz), 2.03 (t, 2H, J = 7.2 Hz), 1.56–1.53 (m, 1H), 1.47–1.42 (m, 3H), 1.28–1.24 (m, 2H). FABMS (+ve) *m/z* 282 [MH$^+$]. HRMS calcd for $C_{13}H_{20}N_3O_2S$ [MH$^+$]: 282.1276. Found: 282.1275.

3.3.11. Biotinamidohexanoyl-6-amino-hexanoyl propargylamide (18b). To biotinamidohexanoyl-6-amino-hexanoic acid *N*-hydroxysuccinimide active ester (**17b**)[32] (50 mg, 0.088 mmol) in DMF (2.0 mL) were added propargylamine (112 μL, 1.64 mmol) and saturated aqueous sodium bicarbonate solution (0.5 mL), and the reaction mixture was stirred at room temperature (2 days). The mixture was concentrated and directly purified by preparative HPLC (isocratic 5% B over 10 min then a linear gradient from 5% B to 40% B over 25 min; retention time = 32.4 min) to give **18b** as a white solid following lyophilization (30 mg, 67% yield). ^{1}H NMR (DMSO-d_6) δ 8.16 (s, 1H), 7.65 (br s, 2H), 6.36 (s, 1H), 6.30 (s, 1H), 4.25 (br s, 1H), 4.08 (br s, 1H), 3.78 (dd, 2H, J = 2.0 Hz, 5.2 Hz), 3.05–3.03 (m, 1H), 3.02 (t, 1H, J = 2.4 Hz), 2.95–2.94 (m, 4H), 2.77 (dd, 1H, J = 4.8 Hz, 12.4 Hz), 2.53 (d, 1H, J = 12.4 Hz), 2.03–1.95 (m, 6H), 1.60–1.52 (m, 1H), 1.48–1.38 (m, 7H), 1.31–1.25 (m, 6H), 1.17–1.16 (m, 4H). FABMS (+ve) *m/z* 508 [MH$^+$]. HRMS calcd for $C_{25}H_{42}N_5O_4S$ [MH$^+$]: 508.2958. Found: 508.2977.

3.3.12. Biotinylated photoprobe ethyl ester (19a). To azide-containing DKA**13** (16 mg, 0.042 mmol) and biotin-containing **18a** (16 mg, 0.057) in *tert*-butanol (0.1 mL) and *N*,*N*-diisopropylethylamine (DIPEA) (0.1 mL) were added freshly prepared ascorbate, 1.0 M in H_2O, (0.8 mL, 0.8 mmol) and copper sulfate pentahydrate, 0.3 M in H_2O (0.3 mL, 0.09 mmol). The heterogeneous mixture was stirred vigorously at room temperature (24 h), then concentrated under reduced pressure and subjected to preparative HPLC purification (linear gradient of 5% B to 100% B over 35 min; retention time = 25.2 min) to provide **19a** as a white solid following lyophilization (5 mg, 18% yield). ^{1}H NMR ($CDCl_3$) δ 8.34 (t, 1H, J = 1.6 Hz), 8.18 (dt, 1H, J = 1.6 Hz, 8.4 Hz), 7.96 (dt, 1H, J = 1.6 Hz, 6.0 Hz),

7.76 (d, 2H, J = 8.4 Hz), 7.72 (s, 1H), 7.62 (t, 1H, J = 7.8 Hz), 7.38 (d, 2H, J = 8.4 Hz), 7.06 (s, 1H), 6.96 (t, 1H, J = 5.6 Hz), 5.58 (d, 2H, J = 3.6 Hz), 4.58–4.51 (m, 2 H), 4.39 (t, 2H, J = 8.0 Hz), 4.38 (dd, 2H, J = 7.2 Hz, 14.4 Hz), 3.13 (dd, 1H, J = 4.8 Hz, 7.6 Hz), 2.91 (dd, 1H, J = 4.8 Hz, 13.4 Hz), 2.73 (d, 1H, J = 13.4 Hz), 2.28–2.17 (m, 2H), 1.68–1.55 (m, 2H), 1.44–1.40 (m, 2H), 1.38 (t, 3H, J = 7.2 Hz), 0.84–0.81 (m, 2H). FABMS (+ve) m/z 661 [MH^+]. FABMS (−ve) m/z 659 [$(M-H)^-$]. HRMS calcd for $C_{33}H_{37}N_6O_7S$ [MH^+]: 661.2439. Found: 661.2415.

3.3.13. Biotinylated photoprobe ethyl ester (19b). Reaction of biotin-containing **18b** (19 mg, 0.037 mmol) and azide-containing DKA **13** in a fashion similar to that reported for the synthesis of **19a** followed by preparative HPLC purification (linear gradient of 5% B to 65% B over 35 min; retention time = 31.4 min) gave **19b** as a white solid following lyophilization (8 mg, 25% yield). ^{1}H NMR (DMSO-d_6) δ 8.32 (d, 1H, J = 8.0 Hz), 8.23 (m, 1H), 7.98 (s, 1H), 7.96 (d, 1H, J = 8.0 Hz), 7.72–7.66 (m, 3H), 7.42 (d, 2H, J = 8.4 Hz), 7.10 (s, 1H), 6.36 (br s, 2H), 5.67 (s, 2H), 4.30–4.24 (m, 5H), 4.09–4.05 (m, 1H), 3.04–3.03 (m, 1H), 2.94–2.93 (m, 4H), 2.76 (dd, 1H, J = 5.2 Hz, 12.8 Hz), 2.52 (d, 1H, J = 12.8 Hz), 2.04–2.01 (m, 2H), 2.00–1.94 (m, 4H), 1.58–1.53 (m, 1H), 1.45–1.39 (m, 7H), 1.34–1.21 (m, 6H), 1.26 (t, 3H, J = 6.8 Hz), 1.18–1.10 (m, 4H). FABMS (+ve) m/z 887 [MH^+]. HRMS calcd for $C_{45}H_{58}N_8O_9NaS$ [$M+Na^+$]: 909.3940. Found: 909.3927.

3.3.14. Biotinylated photoprobe (5a). The ethyl ester **19a** (5 mg, 7.6 μmol) was dissolved in THF (100 μL) with H_2O (100 μL), lithium hydroxyl monohydrate (10 mg, 0.42 mmol) was then added, and the reaction mixture was stirred at room temperature (1 h). The mixture was concentrated under reduced pressure and purified by preparative HPLC (isocratic 5% B over 10 min then linear gradient from 5% B to 100% B over 30 min; retention time = 27.8 min) to give **5a** as a white solid following lyophilization (4 mg, 83% yield). ^{1}H NMR ($CDCl_3$) δ 8.28 (d, 1H, J = 7.6 Hz), 8.19 (d, 1H, J = 7.6 Hz), 8.09 (s, 1H), 7.79 (d, 2H, J = 8.4 Hz), 7.69 (t, 1H, J = 7.6 Hz), 7.66 (s, 1H), 7.43 (d, 2H, J = 8.4 Hz), 6.95 (s, 1H), 6.93 (br s, 1H), 5.61 (d, 2H, J = 2.4 Hz), 4.60–4.54 (m, 2H), 4.47–4.37 (m, 2H), 3.16 (br s, 1H), 2.92 (dd, 1H, J = 4.8 Hz, 13.2 Hz), 2.74 (d, 1H, J = 13.2 Hz), 1.77–1.61 (m, 2H), 1.49–1.46 (m, 2H), 1.27–1.22 (m, 2H), 0.85–0.81 (m, 2H). FABMS (−ve) m/z 631 [$(M-H)^-$]. HRMS calcd for $C_{31}H_{33}N_6O_7S$ [MH^+]: 633.2126. Found: 633.2134.

3.3.15. Biotinylated photoprobe (5b). Compound **19b** (5 mg, 5.6 μmol) was treated in a fashion similar to that used to convert **19a** to **5a**. The product was purified by preparative HPLC (linear gradient from 5% B to 65% B over 35 min; retention time = 26.3 min) to afford **5b** as a white solid following lyophilization (4 mg, 84% yield). ^{1}H NMR (DMSO-d_6) δ 8.31 (d, 1H, J = 7.6 Hz), 8.24 (t, 1H, J = 2.0 Hz), 7.98 (s, 1H), 7.95 (d, 1H, J = 7.6 Hz), 7.73 (d, 2H, J = 8.4 Hz), 7.68–7.63 (m, 1H), 7.42 (d, 2H, J = 8.4 Hz), 7.07 (s, 1H), 6.36 (br s, 1H), 6.30 (br s, 1H), 5.67 (s, 2H), 4.26–4.24 (m, 3H), 4.09–4.05 (m, 1H), 3.06–3.01 (m, 1H), 2.94–2.93 (m, 4H), 2.76 (dd, 1H, J = 5.2 Hz, 12.8 Hz), 2.52 (d, 1H, J = 12.8 Hz), 2.04–1.94 (m, 6H), 1.55–1.53 (m, 1H), 1.43–1.38 (m, 7H), 1.34–1.23 (m, 6H), 1.19–1.14 (m, 4H). FABMS (−ve) m/z 857 [$(M-H)^-$]. HRMS calcd for $C_{43}H_{54}N_8O_9NaS$ [$M+Na^+$]: 881.3627. Found: 881.3628.

Acknowledgments

The authors thank Drs. James A. Kelley and Christopher Lai of the Laboratory of Medicinal Chemistry, NCI, for mass spectral data. This research was supported in part by the Intramural Research Program of the NIH, Center for Cancer Research, National Cancer Institute.

Supplementary data

Supplementary data associated with this article can be found, in the online version, at doi:10.1016/j.bmc.2006.07.064.

References and notes

1. Chiu, T. K.; Davies, D. R. *Curr. Top. Med. Chem.* **2004**, *4*, 965.
2. Hazuda, D. J.; Young, S. D. *Adv. Antiviral Drug Des.* **2004**, *4*, 63.
3. Pommier, Y.; Johnson, A. A.; Marchand, C. *Nat. Rev. Drug Disc.* **2005**, *4*, 236.
4. Marchand, C.; Johnson, A. A.; Semenova, E. A.; Pommier, Y. *Drug Discovery Today: Disease Mechanism*, in press.
5. Semenova, E. A.; Johnson, A. A.; Marchand, C.; Pommier, Y. *Curr. Opin. HIV AIDS*, in press.
6. Witvrouw, M.; Vercammen, F. J.; Maele, B. V.; Engelorghs, Y.; Debyser, Z. *Curr. Med. Chem.—Anti-Infective Agents* **2005**, *4*, 153.
7. Hazuda, D. J.; Felock, P.; Witmer, M.; Wolfe, A.; Stillmock, K.; Grobler, J. A.; Espeseth, A.; Gabryelski, L.; Schleif, W.; Blau, C.; Miller, M. D. *Science* **2000**, *287*, 646.
8. Wai, J. S.; Egbertson, M. S.; Payne, L. S.; Fisher, T. E.; Embrey, M. W.; Tran, L. O.; Melamed, J. Y.; Langford, H. M.; Guare, J. P., Jr.; Zhuang, L.; Grey, V. E.; Vacca, J. P.; Holloway, M. K.; Naylor-Olsen, A. M.; Hazuda, D. J.; Felock, P. J.; Wolfe, A. L.; Stillmock, K. A.; Schleif, W. A.; Gabryelski, L. J.; Young, S. D. *J. Med. Chem.* **2000**, *43*, 4923.
9. Zhang, X.; Pais, G. C. G.; Svarovskaia, E. S.; Marchand, C.; Johnson, A. A.; Karki, R. G.; Nicklaus, M. C.; Pathak, V. K.; Pommier, Y.; Burke, T. R., Jr. *Bioorg. Med. Chem. Lett.* **2003**, *13*, 1215.
10. Goldgur, Y.; Craigie, R.; Cohen, G. H.; Fujiwara, T.; Yoshinaga, T.; Fujishita, T.; Sugimoto, H.; Endo, T.; Murai, H.; Davies, D. R. *Proc. Natl. Acad. Sci. U.S.A.* **1999**, *96*, 13040.
11. Embrey, M. W.; Wai, J. S.; Funk, T. W.; Homnick, C. F.; Perlow, D. S.; Young, S. D.; Vacca, J. P.; Hazuda, D. J.; Felock, P. J.; Stillmock, K. A.; Witmer, M. V.; Moyer, G.; Schleif, W. A.; Gabryelski, L. J.; Jin, L.; Chen, I. W.; Ellis,

J. D.; Wong, B. K.; Lin, J. H.; Leonard, Y. M.; Tsou, N. N.; Zhuang, L. *Bioorg. Med. Chem. Lett.* **2005**, *15*, 4550.
12. Grobler, J. A.; Stillmock, K.; Hu, B.; Witmer, M.; Felock, P.; Espeseth, A. S.; Wolfe, A.; Egbertson, M.; Bourgeois, M.; Melamed, J.; Wai, J. S.; Young, S.; Vacca, J.; Hazuda, D. J. *Proc. Natl. Acad. Sci. U.S.A.* **2002**, *99*, 6661.
13. Hazuda, D. J.; Anthony, N. J.; Gomez, R. P.; Jolly, S. M.; Wai, J. S.; Zhuang, L.; Fisher, T. E.; Embrey, M.; Guare, J. P., Jr.; Egbertson, M. S.; Vacca, J. P.; Huff, J. R.; Felock, P. J.; Witmer, M. V.; Stillmock, K. A.; Danovich, R.; Grobler, J.; Miller, M. D.; Espeseth, A. S.; Jin, L.; Chen, I. W.; Lin, J. H.; Kassahun, K.; Ellis, J. D.; Wong, B. K.; Xu, W.; Pearson, P. G.; Schleif, W. A.; Cortese, R.; Emini, E.; Summa, V.; Holloway, M. K.; Young, S. D. *Proc. Natl. Acad. Sci. U.S.A.* **2004**, *101*, 11233.
14. Parrill, A. L. *Curr. Med. Chem.* **2003**, *10*, 1811.
15. Hatanaka, Y.; Sadakane, Y. *Curr. Top. Med. Chem.* **2002**, *2*, 271.
16. Dorman, G.; Prestich, G. D. *Biochemistry* **1994**, *33*, 5661.
17. Zhao, H.; Neamati, N.; Pommier, Y.; Burke, T. R., Jr. *Heterocycles* **1997**, *45*, 2277.
18. Al-Mawsawi, L. Q.; Fikkert, V.; Dayam, R.; Witvrouw, M., ; Burke, T. R., Jr.; Borchers, C.; Neamati, N. *Proc. Nat. Acad. Sci. U.S.A.* **2006**, *103*, 10080–10085.
19. Zhang, X.; Marchand, C.; Pommier, Y.; Burke, T. R., Jr. *Bioorg. Med. Chem. Lett.* **2004**, *14*, 1205.
20. Frick, W.; Bauer-Schafer, A.; Bauer, J.; Girbig, F.; Corsiero, D.; Heuer, H.; Kramer, W. *Bioorg. Med. Chem.* **2003**, *11*, 1639.
21. Hatanaka, Y.; Hashimoto, M.; Kanaoka, Y. *J. Am. Chem. Soc.* **1998**, *120*, 453.
22. Kan, T.; Tominari, Y.; Morohashi, Y.; Natsugari, H.; Tomita, T.; Iwatsubo, T.; Fukuyama, T. *Chem. Commun.* **2003**, 2244.
23. Kragol, G.; Lumbierres, M.; Palomo, J. M.; Waldmann, H. *Angew. Chem., Int. Ed.* **2004**, *43*, 5839.
24. Lee, M.-R.; Jung, D.-W.; Williams, D.; Shin, I. *Org. Lett.* **2005**, *7*, 5477.
25. Sharpless, K. B.; Kolb, H. C. *Book of Abstracts*, 217th ACS National Meeting, Anaheim, California, March 21–25, 1999; ORGN-105.
26. Rostovtsev, V. V.; Green, L. G.; Fokin, V. V.; Sharpless, K. B. *Angew. Chem., Int. Ed.* **2002**, *41*, 2596.
27. Speers, A. E.; Cravatt, B. F. *Chem. Biol.* **2004**, *11*, 535.
28. Collins, J. C.; Hess, W. W.; Frank, F. J. *Tetrahedron Lett.* **1968**, *30*, 3363.
29. Ratcliffe, R.; Rodehorst, R. J. *J. Org. Chem.* **1970**, *35*, 4000.
30. Wang, X. M.; Hou, X.; Zhou, Z.; Mak, T. C. W.; Wong, H. N. C. *J. Org. Chem.* **1993**, *58*, 7498.
31. Pais, G. C. G.; Zhang, X. C.; Marchand, C.; Neamati, N.; Cowansage, K.; Svarovskaia, E. S.; Pathak, V. K.; Tang, Y.; Nicklaus, M.; Pommier, Y.; Burke, T. R., Jr. *J. Med. Chem.* **2002**, *45*, 3184.
32. Available from Sigma–Aldrich, Corp.
33. Jang, H.; Fafarman, A.; Holub, J. M.; Kirshenbaum, K. *Org. Lett.* **2005**, *7*, 1951.
34. Semenova, E. A.; Johnson, A. A.; Marchand, C.; Davis, D. A.; Yarchoan, R.; Pommier, Y. *Mol. Pharmacol.* **2006**, *69*, 1454.
35. Mazumder, A.; Neamati, N.; Pilon, A. A.; Sunder, S.; Pommier, Y. *J. Biol. Chem.* **1996**, *271*, 27330.
36. Mazumder, A.; Pommier, Y. *Nucleic Acids Res.* **1995**, *23*, 2865.
37. Karki, R.; Tang, Y.; Burke, T. R., Jr.; Nicklaus, M. C. *J. Comput. Aided Mol. Des.* **2004**, *18*, 739.
38. First Discovery 2.0, Schrodinger, Inc., Portland, OR. 2002.
39. Jorgensen, W. L.; Maxwell, D. S.; Tirado-Rives, J. *J. Am. Chem. Soc.* **1996**, *118*, 11225.